# 2D AXISYMMETRIC VS. 3D SOLID ELEMENT PHASE-FIELD DAMAGE MODELING

## Vladimir DUNIĆ[1], Aleksandar BODIĆ[2], Miroslav Živković[3]

[1] 0000-0003-1648-1745, University of Kragujevac Faculty of Engineering, Sestre Janjić 6, Kragujevac, Serbia, E-mail: dunic@kg.ac.rs;

[2] 0000-0002-1713-6540, University of Kragujevac Faculty of Engineering, Sestre Janjić 6, Kragujevac, Serbia, E-mail: abodic@uni.kg.ac.rs;

[3] 0000-0002-0752-6289, University of Kragujevac Faculty of Engineering, Sestre Janjić 6, Kragujevac, Serbia, E-mail: miroslav.zivkovic@kg.ac.rs;

## 1. Introduction

Phase-field damage modeling (PFDM) is very popular among researchers and engineers, because it offers applications to various fields of interest. Investigating damage in structures and predicting its evolution, which can lead to material stiffness degradation and structural failure, is the most interesting aspect. Various research groups at the top world universities have implemented the latest findings into the commercial and research finite element method (FEM) codes, and the PFDM will probably be recognized technique for structural safety monitoring.

However, the practical application is in one of the top interests, but some disadvantages decrease the possibility of efficient and accurate FEM simulations. One of them is the need for a fine FE mesh in the zone where material damage is expected, which makes models with large numbers of degrees of freedom and huge computational time. In this scope, it is important to implement the PFDM for various types of finite elements such as 2D axisymmetric elements, which can decrease the size of the problem by modeling only a cross-section of the axisymmetric structure.

In this paper, we have implemented a previously developed PFDM theory into the 2D axisymmetric element and compared the simulation results to the 3D solid element for the well-known large strain circular bar example.

## 2. Phase-field damage model for 2D axisymmetric element

Recently developed, the critical-total strain based PFDM implementation, presented in [1], was introduced as a user-friendly approach which can be easily applied for simulation of damage evolution in ductile materials. The details are given in several papers published at conferences [2,3] and journals [1,4,5,6], but here, the main equation will be repeated. The internal potential energy consists of elastic, plastic and fracture parts as:

$$W_{int} = W_e + W_p + W_f. \tag{1}$$

The elastic strain energy is:

$$W_e = (1-d)^2 \frac{1}{2} \boldsymbol{\sigma}_0 : \boldsymbol{\varepsilon}_e, \tag{2}$$

where $\boldsymbol{\sigma}_0$ is the Cauchy stress tensor, $\boldsymbol{\varepsilon}_e$ is the elastic strain tensor, and $d$ is damage variable. The plastic part of the internal strain energy is:

$$W_p = (1-d)^2 (\sigma_{yv} \bar{\varepsilon}_p + (\sigma_{y0,\infty} - \sigma_{yv})(\bar{\varepsilon}_p + \frac{1}{n} e^{-n\bar{\varepsilon}_p}) + \frac{1}{2} H \bar{\varepsilon}_p^2), \tag{3}$$

where $\sigma_{yv}$ is the yield stress, $\bar{\varepsilon}_p$ is the equivalent plastic strain, $\sigma_{y0,\infty}$ is the saturation hardening stress, $n$ is the hardening exponent and $H$ is the hardening modulus. The fracture strain energy density is:

$$W_f = G_v[d + \frac{l_c^2}{2} |\nabla d|^2], \tag{4}$$

where $G_v$ is the specific fracture energy per unit volume and $l_c$ is the characteristic length. By derivation of the equilibrium of external and internal potential energy, the final form of the equilibrium equation can be found as:

$$Div\boldsymbol{\sigma} + \boldsymbol{b} = 0. \tag{5}$$

The plasticity yielding condition law is:

$$\bar{\sigma}_{eq} - \sigma_{yv} - (\sigma_{y0,\infty} - \sigma_{yv})(1 - e^{-n\bar{\varepsilon}_p}) - H\bar{\varepsilon}_p = 0. \tag{6}$$

Finally, the phase-field damage evolution law can be derived as:

$$G_v[d - l_c^2 \nabla^2 d] + g'(d)\max(\psi_e + \psi_p - G_v/2) = 0, \tag{7}$$

where $\psi_e$ and $\psi_p$ are the effective elastic and plastic strain energy.

The critical fracture energy $G_v$ can be calculated by finding the effective critical strain energy as $G_v/2$, what gives:

$$G_v = \frac{\sigma_{yv}^2}{E} + 2\sigma_{yv}\left(\varepsilon_{cr} - \frac{\sigma_{yv}}{E}\right) + 2\left(\sigma_{y0,\infty} - \sigma_{yv}\right)\left[\left(\varepsilon_{cr} - \frac{\sigma_{yv}}{E}\right) + \frac{1}{n}\left(e^{-n\varepsilon_{cr}} - e^{-n\frac{\sigma_{yv}}{E}}\right)\right] + H\left(\varepsilon_{cr}^2 - \frac{\sigma_{yv}^2}{E^2}\right). \tag{8}$$

where $\varepsilon_{cr}$ is the critical total equivalent strain, and $E$ is the elasticity modulus.

## 3. Finite element models and material parameters

The presented critical-total strain based PFDM is implemented into the software PAK-DAM v25 [7] for the 3D solid and 2D axisymmetric element. Both implementations can be tested for the well-known circular bar necking example [8]. For that purpose, a large strain von Mises plasticity constitutive model is used and logarithmic strain measure [9].

Dimensions of the half of the bar which is modeled by 2D axisymmetric and 3D solid elements are given as follows: bottom radius is 6.35mm, while the upper side is 1% larger – 6.4135mm, length is 26.67mm. The imperfection is prescribed to trigger the necking at the position where the radius is smaller. The 2D axisymmetric model has 96 elements with mid-side nodes which gives 345 nodes in total.

In Figure 1, the boundary and loading conditions for a 2D axisymmetric finite element model are given. A cross-section of the ¼ of the specimen is modeled, so the y-symmetry boundary conditions are prescribed at the bottom side, while the opposite side is loaded by prescribed displacements which are connected by equations in the y-direction to the node on the central axis. In Figure 2, the same data are given for the 3D solid finite element model. One quarter of the half of the bar is modeled while symmetry boundary conditions are prescribed at appropriate surfaces. On the bottom side, also, the y-symmetry boundary conditions are necessary as well as loading conditions defined by prescribed displacements. The 3D model has 648 finite elements with mid-side nodes, which gives in total of 3388 nodes. As it can be noticed, the 3D model is approximately 10 times larger, and refinement of the mesh for a more detailed simulation is practically impossible.

The simulation is performed by the Full Newton iterative method with line search. The solution is obtained in 40 steps with a displacement increment of 0.2 mm, up to the total displacement of 8 mm.
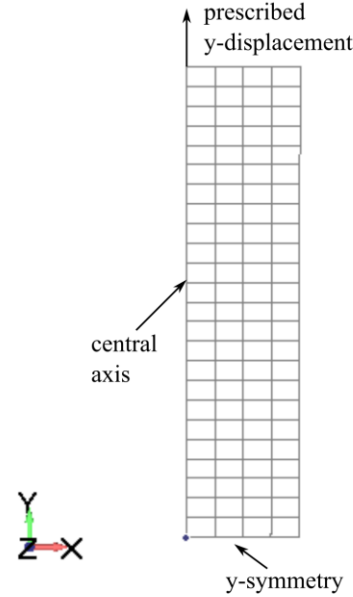


**Fig. 1.** 2D axisymmetric finite element model with boundary and loading conditions.
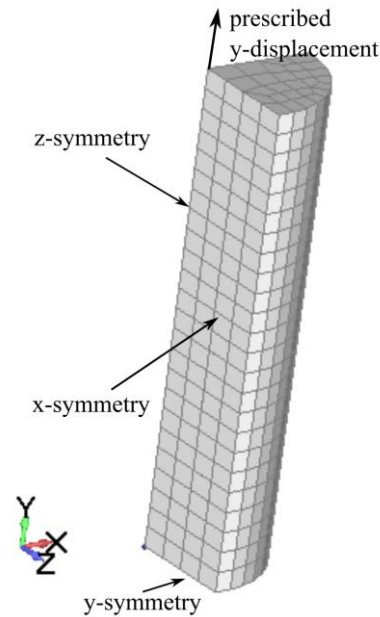


**Fig. 2.** 3D solid finite element model with boundary and loading conditions.

## 4. Simulation results

The simulation is performed to show the functionality of the critical-total strain based PFDM implementation into the both 2D axisymmetric and 3D solid finite elements in PAK-DAM v25 software [7].

**Table 1.** Material parameters

| Parameter | Value | Parameter | Value |
|---|---|---|---|
| Young modulus | 210.4 [GPa] | Exponential hardening | 16.93 [-] |
| Poisson's ratio | 0.3118 [-] | Linear hardening | 0.12924 [-] |
| Yield stress | 0.45 [GPa] | Critical eq. strain | 1.2 [-] |
| Saturation stress | 0.715 [GPa] | Characteristic length | 0.5 [mm] |

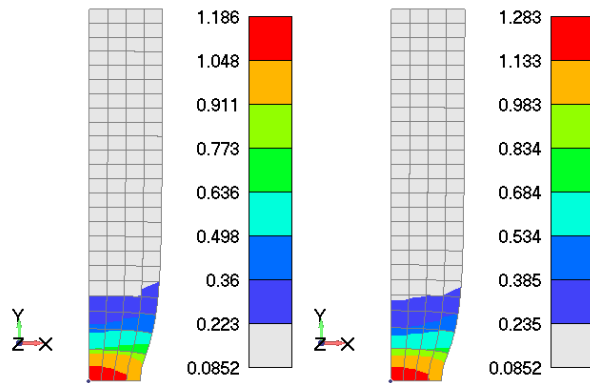In Figure 3, the equivalent plastic strain field is given in 31. and 32. time step, as the critical strain is achieved at that moment.



**Fig. 3.** Equivalent plastic strain field in 31 (left) and 32 (right) time steps for a 2D axisymmetric FE model.

In Figure 4, the damage field is given for the steps 32 and 33, as an important detail which verifies the control over the damage onset by critical equivalent strain.
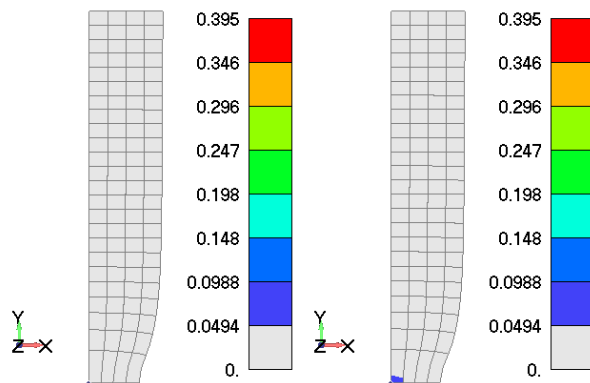


**Fig. 4.** Damage field in 32 (left) and 33 (right) time steps for a 2D axisymmetric FE model.

In Figure 5, the damage field is given for the last time step for both the 3D solid and 2D axisymmetric models to compare the obtained results.

In Figure 6, the equivalent plastic strain field is given for the last time step for both the 3D solid and 2D axisymmetric models to compare the obtained results.
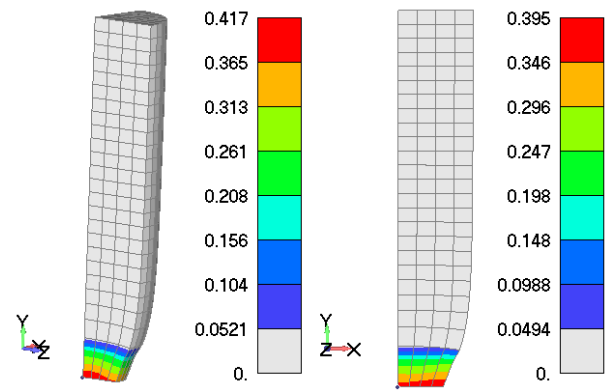


**Fig. 5.** Damage field in the last (40) time step for 3D solid (left) and 2D axisymmetric (right) FE model.
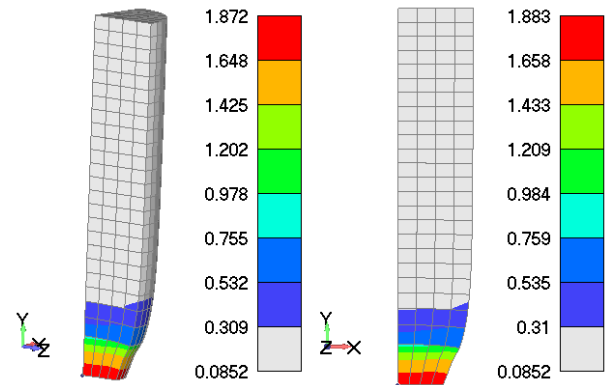


**Fig. 6.** Equivalent plastic strain field in the last (40) time step for 3D solid (left) and 2D axisymmetric (right) FE model.

In Figure 7, the damage field evolution at the end of the simulation is given for the last six time steps for the 2D axisymmetric model.
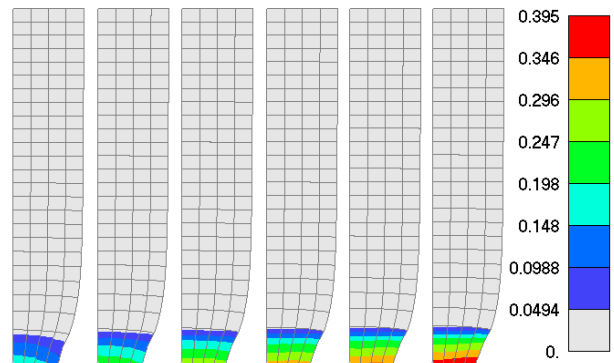


**Fig. 7.** Damage evolution in 2D axisymmetric FE model in the last six time steps (35-40 from left to right) of the simulation.

In Figure 8, the constraint force vs. displacement diagram at the upper side of the model is given for both the 3D solid and 2D axisymmetric models to compare the responses.
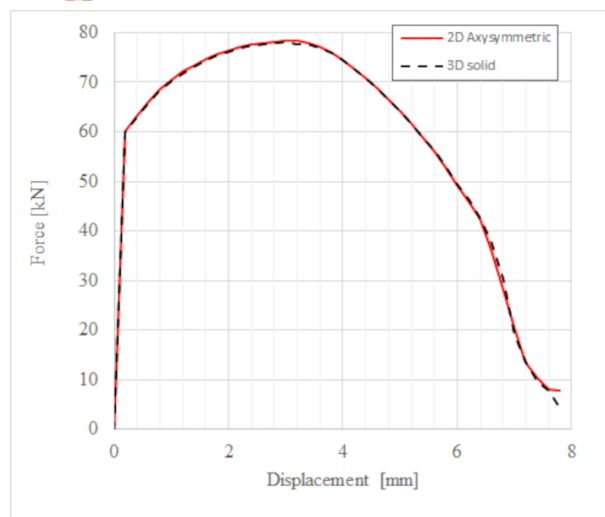
**Fig. 8.** Force-displacement response for 2D axisymmetric and 3D solid FE model

## 5. Discussion and conclusions

The simulation results presented in previous sections offer many points of interest for discussion. Firstly, the material parameters given in Table 1, define the stress-strain response of the material, but one important parameter for the PFDM simulation is the critical equivalent strain which is set to 1.2. As, the equivalent plastic strain defines the yield stress function in eq. (6), when the critical value is reached in time step 32 (Figure 3.), in the next time step 33, the damage occurs (Figure 4.). It is one time step later because the solution procedure is defined in a partitioned manner, so the damage field is late for one time step with respect to the displacement field. In Figure 5, it can be seen that the damage field achieves a similar level for both 2D axisymmetric and 3D solid FE models, but small difference (less than 5%) can be noticed. A similar situation is for the equivalent plastic strain field at the last time step, given in Figure 6, but the difference is less than 1%. Figure 7 shows the evolution of the damage field in the specimen across the cross-section in the necking zone. Although, relatively coarse mesh is used, the increase of damage zone can be observed. Finally, in Figure 8, the force-displacement response of the circular bar model is compared for the 3D solid and 2D axisymmetric FE models and the overlapping of the diagrams is obvious.

At the end, by analyzing the obtained results, it can be confirmed that both implementations of PFDM are functional and that the proposed method can be used for real structures. In this case, large strain nonlinear analysis with the Von Mises plasticity model and exponential hardening function is used, which is one of the most advanced simulations in the field. Of course, the advantage of a 2D axisymmetric finite element is obvious for the computational time necessary to solve the problem, but for detailed analysis, the 3D solid element can be used successfully.

## Acknowledgments

## References

[1] Dunić, V., Gubeljak, N., Živković, M., Milovanović, V., Jagarinec, D., Djordjevic, N. Experimental Characterization and Phase-Field Damage Modeling of Ductile Fracture in AISI 316L, *Metals*, 2024, 14(7), 787.

[2] Dunić, V., Živković, M., Milovanović, V. Phase-field Fatigue modeling in ductile materials, *The 9th European Congress on Computational Methods in Applied Sciences and Engineering - ECCOMAS 2024*, Lisbon, Portugal, 3-7 June 2024. (e-source)

[3] Dunić, V., Živković, M.; Critical total-strain based Phase-Field Damage Model implementation for ductile fatigue, *5th International Conference on Computational Engineering ICCE 2024*, Darmstadt, Germany, 30 September-2 October 2024. (e-source)

[4] Dunić, V., Živković, J., Milovanović, V., Pavlović, A., Radovanović, A., Živković, M. Two-Intervals Hardening Function in a Phase-Field Damage Model for the Simulation of Aluminum Alloy Ductile Behavior, Metals, 2021, 11(11), 1685.

[5] Živković, J., Dunić, V., Milovanović, V., Pavlović, A., Živković, M. A Modified Phase-Field Damage Model for Metal Plasticity at Finite Strains: Numerical Development and Experimental Validation, Metals, 2021, 11(1), 47.

[6] Miehe, C., Welschinger, F., Hofacker, M. Thermodynamically consistent phase-field models of fracture: Variational principles and multi-field FE implementations. Int. J. Numer. Methods Eng. 2010, 83, 1273–1311.

[7] Živković, M., Dunić, V., Rakić, D., Grujović, N., Slavković, R., Kojić, M. PAK-DAM Software for Damage and Fracture Simulation; Faculty of Engineering, University of Kragujevac: Kragujevac, Serbia, 2025.

[8] Simo, J.C., Miehe, C. Associative coupled thermoplasticity at finite strains: Formulation, numerical analysis and implementation. *Comput. Methods Appl. Mech. Eng.* 1992, 98, 41–104.

[9] Kojić, M., Bathe, K.J. *Inelastic Analysis of Solids and Structures*, Springer: Berlin/Heidelberg, Germany, 2005.